Free Radical Research, December 2005; 39(12): 1335–1344

Taylor & Francis
Taylor & Francis Group

Proteomic characterization of oxidative dysfunction in human umbilical vein endothelial cells (HUVEC) induced by exposure to oxidized LDL

TOMOYA KINUMI[1], YOKO OGAWA[1], JUNKO KIMATA[1,2], YOSHIRO SAITO[1], YASUKAZU YOSHIDA[1], & ETSUO NIKI[1]

[1]*Human Stress Signal Research Center (HSSRC), National Institute of Advanced Industrial Science and Technology (AIST), Ikeda, Osaka 563-8577, Japan, and* [2]*Thermo Electron K.K., C-2F, Moriya-cho, Kanagawa-ku, Yokohama 221-0022, Japan*

Accepted by Professor N. Taniguchi

(Received 1 August 2005)

Abstract

The oxidative modification of low-density lipoprotein (LDL) and subsequent alteration of endothelial cell function are generally accepted as an important early event in the pathogenesis of atherosclerosis. To understand the mechanism by which oxidized LDL (oxLDL) causes dysfunction in endothelial cells, human umbilical vein endothelial cells (HUVEC) were exposed to oxLDL at a concentration that induces cellular dysfunction, and proteomic analysis was carried out, together with the analysis of cellular lipid peroxidation products. Time-dependent accumulation of 7-ketocholesterol and the progression of oxidative modification of peroxiredoxin 2 were observed, together with the suppression of cell proliferation. Proteomic analysis using two-dimensional gel electrophoresis (2-D gel) revealed that nucleophosmin, stathmin, and nucleolin were differentially expressed after exposure to oxLDL. Both 2-D gel and western blot analyses revealed that (1) nucleophosmin was dephosphorylated in a time-dependent manner; (2) stathmin was transiently phosphorylated at 6 h, and the unphosphorylated form was continuously down-regulated; and (3) nucleolin was identified as a 20-kDa fragment and a 76-kDa form, which were down-regulated. These observations suggest that the exposure of HUVEC to oxLDL results in the suppression of cell proliferation, which is ascribed to protein modification and/or altered expression of nucleophosmin, stathmin, and nucleolin under these oxidative stress conditions.

Keywords: *Endothelial cell, lipid peroxidation, oxidative stress, oxidized LDL, proteome*

Abbreviations: *AAPH, 2,2′-azobis(2-amidinopropane) dihydrochloride; AIPH, 2,2′-azobis(2-[2-imidazolin-2-yl]propane) dihydrochloride; CE, cholesteryl ester; CEOH, cholesteryl ester hydroxide; CEOOH, cholesteryl ester hydroperoxide; CEO(O)H, cholesteryl ester hydroxide and hydroperoxide; CHAPS, 3-([3-cholamidopropyl] dimethylammonio)-1-propane sulfonate; 2-D gel, two-dimensional gel electrophoresis; DTT, dithiothreitol; EDTA, ethylenediaminetetraacetic acid; Ch, free cholesterol; 7-KCh, 7-ketocholesterol; 7-OHCh, 7-hydroxycholesterol; HNE, 4-hydroxynonenal; 7-OOHCh, cholesterol 7-hydroperoxide; HUVEC, human umbilical vein endothelial cells; HPLC, high-performance liquid chromatography; LDL, low-density lipoprotein; nano-ESI, nano-electrospray ionization; nonospray HPLC-MS/MS, nanospray interface capillary HPLC-electrospray ionization/tandem mass spectrometry; MS/MS, tandem mass spectrometry; MTT, 3-(4,5-dimethylthiazol-2-yl)-2, 5-diphenyltetrazolium bromide; oxLDL, oxidized low-density lipoprotein; oxPrx, oxidatively modified peroxiredoxin; PBS, phosphate-buffered saline; PC, phosphatidylcholine; PCOH, phosphatidylcholine hydroxide; PCOOH, phosphatidylcholine hydroperoxide; PCO(O)H, phosphatidylcholine hydroxide and hydroperoxide; pI, isoelectric point; Prx, peroxiredoxin; SDS, sodium dodecyl sulfate; SDS-PAGE, sodium dodecyl sulfate-polyacrylamide gel electrophoresis; TFA, trifluoroacetic acid*

Introduction

The role of free radicals in biology has been the subject of extensive studies in relation to oxidative stress and cellular signaling. It is now accepted that at high concentrations, free radicals are hazardous. The dysfunction of lipids, proteins, and nucleic acid molecules under these conditions is implicated in various degenerative diseases

Correspondence: Tomoya Kinumi, HSSRC, AIST, 1-8-31 Midorigaoka, Ikeda, Osaka 563-8577, Japan. Tel: +81 72 751 8242. Fax: +81 72 751 9964. E-mail: t.kinumi@aist.go.jp

ISSN 1071-5762 print/ISSN 1029-2470 online © 2005 Taylor & Francis
DOI: 10.1080/10715760500306695

such as neurodegenerative diseases, atherosclerosis, and cancer [1]. The oxidative modification of low-density lipoprotein (LDL) is an important initial event in the pathogenesis of atherosclerosis [2]. Accordingly, there are many studies of oxidized LDL (oxLDL) reported. For example, oxLDL can stimulate vascular smooth muscle cell (VSMC) proliferation under cell culture conditions [3] and exerts growth-promoting effects on cells *in vitro*, including the induction of transcription factors [4] and the enzymes involved in mitogenesis [5]. On the other hand, some researchers have reported that components of oxLDL such as lysophosphatidylcholine (lysoPC) [6], 7-ketocholesterol (7-KCh) [7], and 4-hydroxynonenal (HNE) [8] induce the dysfunction and apoptosis of cultured endothelial cells. However, the effects of oxLDL on the major cell types within atherosclerotic lesions (endothelial cells, smooth muscle cells, macrophages, and lymphocytes) are still not known in detail.

In a recent proteomic study, two-dimensional gel electrophoresis (2-D gel) of mammalian cells revealed that the isoelectric points (pIs) of several protein spots showed acidic mobility shift under oxidative stress [9,10]. In those studies, several oxidative stress responsive proteins, such as five of the subclasses of peroxiredoxins (peroxiredoxins 1, 2, 3, 4, and 6) and DJ-1, were identified within a variety of cultured cells and with stressors, such as hydrogen peroxide and paraquat [11,12]. Although many works have reported oxLDL and its effects on the major cell types within atherosclerotic lesions, only a few proteomic studies have extensively characterized cells exposed to oxLDL. Fach et al. reported the proteomic analysis of an in vitro foam cell model treated with oxidized LDL using differentiated human THP1 cells as a macrophage model system [13]. They identified a set of prospective biomarkers of atherosclerosis, involving seven families of proteins: Fatty acid-binding proteins, chitinase-like enzymes, cyclophilins, cathepsins, proteoglycans, urokinase-type plasminogen activator receptor, and a macrophage scavenger receptor. Another research group reported the proteomic analysis of oxLDL-exposed endothelial cells to elucidate the effects of the isoflavone genistein [14,15].

In the present study, to mimic atherosclerotic lesions, human umbilical vein endothelial cells (HUVEC) were exposed to oxLDL at a concentration that induces cellular dysfunction and extensive analyses of both the proteomics and lipid peroxidation products were carried out. This comprehensive analysis of cellular proteins and lipids makes available valuable information regarding cellular responses to oxLDL.

Materials and methods

Oxidation of LDL

After an overnight fast, blood from a healthy donor (41 years old male) was collected in ethylenediaminetetraacetic acid (EDTA)-containing tubes. The samples were immediately placed on ice after collection. Plasma was separated by centrifugation at 3000*g* for 10 min at 4°C and used immediately. LDL was separated from the plasma by ultra-centrifugation as described in the literature [16] within a density cutoff of 1.019–1.063 g/ml, and then dialyzed for 12 h in cellulose membranes against phosphate-buffered saline (PBS, pH 7.4) containing 100 μM EDTA. The protein concentration of LDL was measured using the bicinchonic acid protein assay reagent (Pierce, Rockford, IL, USA). Oxidation of LDL (1.50 mg protein/ml) was carried out at 37°C under air for 12 h. Oxidation was initiated by the addition of 1 mM 2,2′-azobis(2-[2-imidazolin-2-yl]propane) dihydrochloride (AIPH; Wako Pure Chemical, Osaka, Japan) dissolved in PBS (1/100 volume to reaction solution). Oxidized LDL was dialyzed for 12 h in cellulose membranes against PBS (pH 7.4) containing 100 μM EDTA to remove AIPH from the LDL.

HPLC analyses

The mixture of oxidized samples was extracted with two volumes of chloroform/methanol (2/1, v/v), and the chloroform layer was injected into an HPLC to analyze its α-tocopherol and lipid hydroperoxide content. Cells were collected and also subjected to lipid hydroperoxide analysis. Antioxidants and lipids were extracted with chloroform/methanol (2/1, v/v). Vitamin E was measured using HPLC with an amperometric electrochemical detector (NANOSPACE SI-1, Shiseido, Tokyo, Japan) set at 800 mV, with an ODS column (LC-18, 5 μm, 250 × 4.6 mm, Supelco, Tokyo, Japan) and methanol/*tert*-butyl alcohol (95/5, v/v) containing 50 mM sodium perchlorate as eluent at a flow rate of 1 ml/min. The plasma level of ascorbic acid was measured by HPLC with a UV detector at 263 nm (SPD-10AV, Shimadzu, Kyoto, Japan). An NH_2 column (Wakosil 5NH_2, 5 μm, 250 × 4.6 mm, Osaka, Japan) was used with 40 mM PBS/methanol (1/9, v/v) as eluent at 1 ml/min. Plasma was diluted with methanol (1/4, v/v) and mixed vigorously with a vortex mixer for 1 min, then centrifuged at 15000 rpm, for 10 min. An aliquot of the upper layer was injected immediately into the HPLC. The concentrations of free cholesterol hydroperoxide (7-OOHCh), 7-ketocholesterol (7-KCh), 7-hydroxycholesterol (7-OHCh), and phosphatidylcholine hydroperoxides (PCOOH) were determined with HPLC using a post-column chemiluminescence detector (CLD-10A, Shimadzu, for 7-OOHCh and PCOOH analyses) and a spectrophotometric detector (SPD-10AV, Shimadzu) at 210 nm (for 7-OHCh analysis) and 245 nm (for 7-KCh) analysis. An ODS-2 column (5 μm, 250 × 4.6 mm, GL Science, Tokyo, Japan) was used with methanol/acetonitrile/water (45/46/9, v/v/v) as eluent at a flow rate of 1 ml/min and after passage through the UV detector, the

eluent was mixed with a luminescent reagent in the post-column mixing joint of the chemiluminescence detector (Shimadzu) at 40°C. The luminescent reagent, containing cytochrome *c* (10 mg) and luminol (2 mg) in 1 L alkaline borate buffer (pH 10), was loaded at a flow rate of 0.5 ml/min. The combined concentrations of cholesteryl ester hydroxides and hydroperoxides (CEO[O]H) were also determined with HPLC using a spectrophotometric detector (SPD-10AV, Shimadzu) at 234 nm. An ODS column (LC-18, 5 μm, 250 × 4.6 mm, Supelco) was used with acetonitrile/isopropyl alcohol/water (44/54/2, v/v/v) as eluent at a flow rate of 1 ml/min.

Cell culture, measurement of cell numbers and cell viability

HUVEC were purchased from Cambrex (Walkersville, MD, USA) and cultured in EGM-2 (Cambrex) containing endothelial cells growth factors with 2% fetal bovine serum at 37°C in a 5% CO_2 atmosphere. All experiments were performed after four passages. To quantify the numbers of cells in six-well culture plates after treatment with LDL or oxLDL, the cells were trypsinized and counted in a hemocytometer. A minimum of 500 cells were counted per treatment. To determine cell viability, an MTT (3-[4,5-dimethylthiazol-2-yl]-2, 5-di-phenyltetrazolium bromide) assay was conducted. The cells were incubated with 0.5 mg/ml MTT at 37°C for 2 h. Isopropyl alcohol containing 0.04 N HCl was added to the culture medium (3/2, v/v), and mixed with a pipette until the formazan was completely dissolved. The optical density of formazan was measured at 570 nm using a Multiskan Ascent plate reader (Thermo Electron, Bellefonte, PA, USA).

Two-dimensional gel electrophoresis and gel image analysis

After treatment with oxidized LDL, cells were washed with PBS, harvested, then dissolved in isoelectric focusing sample buffer consisting of 9 M urea, 2% 3-[(3-cholamidopropyl) dimethylammonio]-1-propane sulfonate (CHAPS) (w/v), 65 mM dithioerythritol (DTE), 0.5% carrier ampholyte (v/v; pH 4–7; Amersham Biosciences, Uppsala, Sweden), 0.5% pepstatin (w/v), 5% benzamidine (w/v), 0.25% leupeptin (w/v), and 1% phosphatase inhibitor cocktail 1 (v/v; P2850, Sigma, St Louis, MO, USA). Protein amounts were quantified with an RC DC Protein Assay kit (Bio-Rad Laboratories, Hercules, CA, USA). The sample solution containing 100 μg of protein was applied to an immobilized pH gradient gel (13 cm, pH 4–7; Amersham Biosciences) and rehydrated for 12 h. Isoelectric focusing was performed for a total of 48990 Vh at a maximum voltage of 8000 V. Each strip was equilibrated in two steps, in 50 mM Tris–HCl (pH 8.8), 6 M urea, 2% sodium dodecyl sulfate (SDS; w/v) and 30% glycerol (v/v), supplemented with 10 mg/ml dithiothreitol (DTT) and 40 mg/ml iodoacetamide, for 20 min each. The second dimension was carried out by 12.5% SDS polyacrylamide gel electrophoresis (SDS-PAGE). Gels were stained with SYPRO Ruby (Bio-Rad Laboratories) and scanned with a Molecular Imager FX (Bio-Rad Laboratories). Image analysis of the scanned gels was performed using Phoretix 2-D software (Nonlinear Dynamics Ltd., UK). Background subtraction and volume normalization were performed automatically by the software. Three independent runs of gels were compared.

In-gel enzymatic digestion and mass spectrometry

Excised spots were washed twice with 100 mM ammonium bicarbonate (pH 8.8), then dehydrated with acetonitrile. The gel pieces were rehydrated in 10 mM DTT-ammonium bicarbonate solution and alkylated with 50 mM iodoacetamide. After dehydration with acetonitrile, the gel pieces were rehydrated on ice for 10 min in 20 μl of 20 mM ammonium bicarbonate containing 50 ng/μl sequence-grade modified trypsin (Promega, Madison, WI, USA). The rehydrated gel pieces were replaced with 20 μl of 20 mM ammonium bicarbonate, and in-gel digestion was performed for 15 h at 37°C. The resulting peptides were extracted twice with 20 μl of 20 mM ammonium bicarbonate and then three times in 20 μl of 0.5% trifluoroacetic acid (TFA) in 50% acetonitrile. The extracts were concentrated to 20 μl with a SpeedVac concentrator (Thermo Electron). The samples were injected into a reversed-phase trap cartridge (CapTrap, Michrom BioResources, Auburn, CA, USA) equipped in an autosampler (HTC PAL, CTC Analytics AG, Switzerland). The cartridge was washed with 0.1% TFA/H_2O, then automatically switched to an HPLC flow line by a 10-port switching valve. A capillary HPLC system (Magic2002, Michrom BioResources) was coupled on-line to a nano-electrospray ionization (nano-ESI) ion trap mass spectrometer (LCQ DECA, Thermo Electron) through the autosampler equipped with the trap cartridge. Chromatographic separations were conducted on a reversed phase capillary column (MAGIC C18, 0.2 mm i.d., 50 mm length; Michrom BioResources) at a flow rate of 2 μl/min which was reduced from the 50 μl/min HPLC flow rate with a precolumn flow splitter. The gradient profile consisted of a linear gradient from 5% solvent B (H_2O/acetonitrile/formic acid, 10/90/0.1, v/v/v) to 65% B in 40 min against solvent A (H_2O/acetonitrile/formic acid, 98/2/0.1, v/v/v). Nano-ESI was performed using a fused silica spray tip of 20 mm length and 20 μm i.d. (PicoTip, New Objective, Woburn, MA, USA) by applying 1.8 kV spray voltage. Data-dependent MS/MS spectra were acquired and converted into DTA file format to be submitted to the MASCOT search software (Matrix Science, London, UK). NCBI and Swiss-Prot were the protein databases used.

Western blot analysis

Proteins separated by SDS-PAGE or 2-D gel were transferred to polyvinylidene fluoride membrane (ProBlott, Applied Biosystems, Foster City, CA, USA), blocked with BlockAce (Dainippon Pharmaceutical Co Ltd., Osaka, Japan), and incubated with a primary antibody in 50 mM Tris–HCl (pH 7.5), 150 mM NaCl, 0.1% Tween 20 (TBS-T). The antibodies used were: polyclonal anti-Prx2 (LabFrontier, Seoul, Korea), monoclonal anti-nucleophosmin (clone #FC-61991; Zymed Laboratories, South San Francisco, CA, USA), polyclonal anti-stathmin (Cell Signaling Technology, Beverly, MA, USA), monoclonal anti-nucleolin (clone #4E2; Medical & Biological Laboratories, Nagoya, Japan), monoclonal anti-DJ-1 (clone #3E8; Medical & Biological Laboratories) and monoclonal anti-actin (clone #C4, Chemicon, Temecula, CA, USA). The membranes were washed three times with TBST, and incubated with peroxidase-conjugated secondary antibody. The specific spot or band was visualized with an ECL western blotting detection system (Amersham Biosciences).

Statistical analysis and reproducibility

The experiments were repeated, in general, several times and the results were reproducible. The numbers of experiments are shown in the figure captions.

Results

Oxidation of LDL and exposure of HUVEC to oxLDL

Human LDL was oxidized by the radical initiator, AIPH (1 mM), which decomposes to form radicals at a constant rate [17]. It decomposes four times faster than 2,2′-azobis(2-amidinopropane) dihydrochloride (AAPH), a frequently used water-soluble radical initiator. The major oxidized products and concentrations are shown in Figure 1(A). Remained AIPH was removed easily from the solution by dialysis for 12 h. In fact, consecutive oxidation was not observed after dialysis, even at the room temperature for several hours (data not shown). No antioxidant, such as α-tocopherol or ascorbic acid, was detected in oxLDL by HPLC analysis after dialysis.

Two hundreds micro liter of an aliquot of oxLDL which contains 370 μM of total oxidized products was then applied to HUVEC in 3 ml culture medium. The final concentration of total oxidized product in the medium was 25 μM and was calculated to be 58 nmol per mg of cell protein. The concentration of total oxidized products used here was calculated as the combined concentrations of the following oxidized lipids: 7-OOHCh, 7-KCh, PCOOH, PCOH, CEOOH, and CEOH. A final concentration of 25 μM was used to investigate the dysfunction of HUVEC,

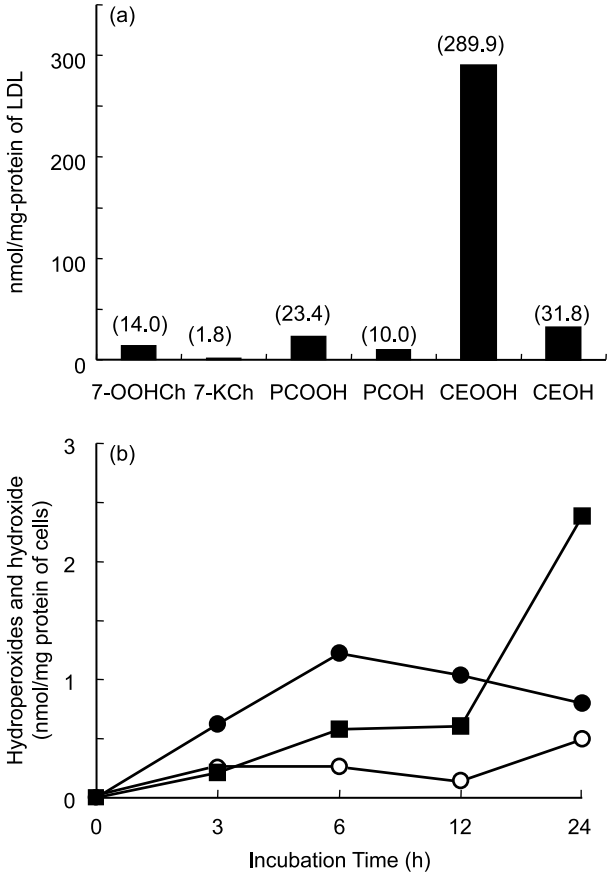

Figure 1. (A) Formation of hydroperoxides and hydroxides in the oxidation of LDL induced by 1 mM AIPH in PBS (pH 7.4) at 37°C in air for 12 h. The parentheses shown in the panel indicate the contents of hydroperoxides or hydroxides in nmol/mg of LDL protein. (B) The increase in cellular CEOOH (•), CEOH (○), and 7-KCh (■) in HUVEC exposed to oxidized LDL at a final concentration of 25 μM hydroperoxides and hydroxides. Data represent typical results of two independent experiments.

because this condition led reproducibly to the suppression of cellular proliferation. As shown in Figure 1(B), a remarkable increase in cellular levels of CEOOH, CEOH, and 7-KCh was observed. The concentrations of CEOOH and CEOH were 0.80 and 0.50 nmol/mg of cell protein, respectively (24 h after exposure), which are equivalent to 3.37 and 16.9% of the initial amounts of added CEOOH and CEOH, respectively. One interpretation of this result is that CEOOH was reduced by cellular phospholipid hydroperoxide glutathione peroxidase (PH-GPx) [18]. Since there was no polyunsaturated CE detected in either intact or oxLDL-exposed HUVEC, the CEOOH and CEOH detected in HUVEC are considered to have been incorporated from the medium. In contrast, the cellular content of 7-KCh (2.38 nmol/mg of cell protein, 24 h after exposure) was five times higher than the amount loaded initially (0.46 nmol/mg of cell protein). No other oxidized products, PCOOH, PCOH, or 7-OOHCh, were detected in the HUVEC.

Suppression of cell proliferation by oxLDL

The effect of oxLDL on the proliferation of HUVEC was assessed by total cell counts. Figure 2 shows that the exposure of cells to oxLDL decreased cell growth to half that of LDL-treated cells. The doubling time of cells with no chemical treatment was 18 h, which is in good agreement with that of cells treated with intact LDL. Cell viability was slightly decreased to 90% after 24 h of oxLDL treatment, whereas treatment with intact LDL caused no decrease in cell viability (data not shown), as assessed by an MTT (3-[4,5-dimethylthiazol-2-yl]-2, 5-di-phenyltetrazolium bromide) assay. Total cell counts and MTT assays showed that the treatment of cells with oxLDL resulted in significant suppression of cell growth compared with that of LDL-treated controls.

Proteomic analysis of HUVEC treated with LDL or oxLDL

Total cell lysates were analyzed in triplicate by 2-D gel, using 13 cm, pI 4–7 isoelectric focusing gels in the first dimension and 16 cm, 12.5% SDS-PAGE in the second dimension. Proteins were visualized by fluorescence staining using SYPRO Ruby, which resolved about 700 distinct protein spots. Figure 3 shows a representative 2-D gel of HUVEC. Three protein spots differed in density in samples from control cells and oxLDL-treated cells, based on differences in their normalized and averaged intensities on triplicate 2-D gels. We also examined the redox-sensitive proteins, Prx2 and DJ-1 as intracellular redox markers. The three differentially expressed protein spots (marked 1–3 in Figure 3) and the two tentatively identified specific protein spots (marked 4 and 5 in Figure 3) were processed

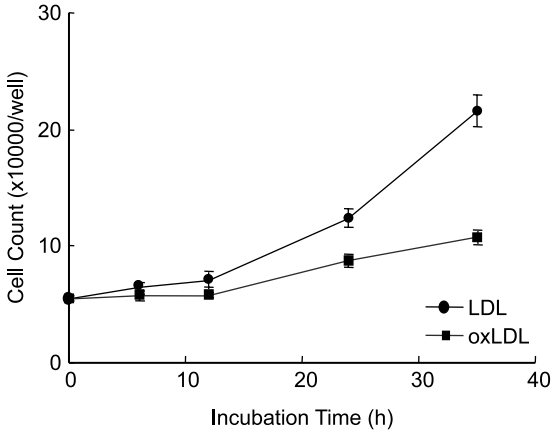

Figure 2. Cell counts of HUVEC that were exposed to oxidized LDL (■) at a final concentration of 25 μM hydroperoxides and hydroxides, or to intact LDL (•) that contained protein equivalent to the amount in the oxidized LDL. Cells were counted using a hemocytometer and the numbers were given as means ± SD ($n = 4$).

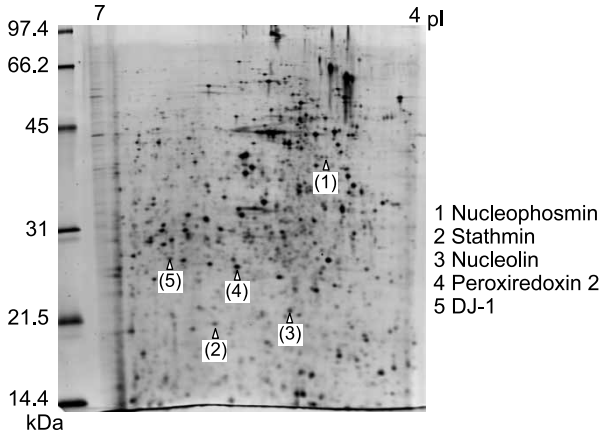

Figure 3. Representative 2-D gel image of HUVEC whole cell lysate, when 100 μg of cell protein was used in the analysis. The gel was visualized by fluorescence staining with SYPRO Ruby.

by in-gel trypsin digestion and analyzed by nanospray HPLC-MS/MS. The sets of mass spectra and tandem mass spectra of in-gel tryptic digests were searched by peptide mass fingerprinting and MS/MS searches against non-redundant human sequence databases. The results are summarized in Table I. The identification of these five protein spots was further investigated by western blot analysis using specific antibodies, because these proteins possibly exist as several isoforms due to post-translational modifications such as phosphorylation and cysteine oxidation.

No difference in Prx2 (spot 4) or DJ-1 (spot 5) caused by exposure to oxLDL was observed on fluorescence stained 2-D gel relative to the LDL-treated controls. However, as we have previously reported, Prx2 and DJ-1 undergo an acidic shift of pI under oxidative stress conditions [19]. In fact, western blot analysis revealed that Prx2 gave a single spot under control conditions, whereas it appeared as a more acidic spot under conditions of oxidative stress generated by exposure of the cells to oxLDL (Figure 4(A)). The acidic spot was identified as oxidatively modified Prx2 (oxPrx2) and the acidic spot shift was confirmed to be due to the oxidation of an active cysteine residue to cysteine sulphinic acid (Cys-SO_2H) and/or cysteine sulfonic acid (Cys-SO_3H) [20]. The pI of the basic Prx2 spot on 2-D gel was 5.8, which is in good agreement with the theoretical pI (5.7), whereas the acidic satellite of Prx2 had a pI of 5.4. As shown in Figure 4(B), the spot density of oxPrx2 measured by western blot analysis in Figure 4(A) increased with increasing incubation time with oxLDL. This observation suggests a progressive oxidative modification of HUVEC. On the other hand, DJ-1 was not modified by this stimulation, probably because the oxidative modification of DJ-1 is less easy to achieve than that of Prx2 [11,19].

Table I. Protein identified by LC-MS/MS corresponding to the spots on 2-D gel.

Spot No.	Name of protein	Observed		Theoretical		Accession No		Sequence coverage (%)
		pI	mass (kDa)	pI	MW	NCBI	Swiss prot	
1	Nucleophosmin	4.9	36.5	4.6	32726	gi|30582861	P06748	31
2	Stathmin	6.0	20.3	5.8	17161	gi|57528035	P16949	36
3	Nucleolin	5.2	20.8	4.6	76224	gi|128841	P19338	12
4	Peroxiredoxin 2	5.8	23.0	5.7	22049	gi|2507169	P32119	27
5	DJ-1	6.5	23.4	6.3	19878	gi|31543380	Q99497	33

As shown in Figure 5, the density of spot 1 (nucleophosmin) was increased by oxLDL in a time-dependent manner, whereas the two spots corresponding to stathmin (spot 2) and nucleolin (spot 3) decreased in density after exposure to oxLDL. These proteins are involved in important cellular processes such as cell proliferation. We also used western blot analysis to investigate the post-translational modifications of these three proteins, which may be altered by exposure to oxLDL.

As shown in Figure 6, western blot analysis of nucleophosmin showed a variety of spots corresponding to nucleophosmin isoforms. The distributed pattern of nucleophosmin isoforms is due to their phosphorylation [21]. However, details of their structures, e.g. their phosphorylation sites, were not fully determined. The set of distributed spots marked by brackets was shifted to its basic side, suggesting that their dephosphorylation occurred in a time-dependent manner, whereas the spot indicated by arrowheads increased in intensity after exposure to oxLDL. One isoform of nucleophosmin on fluorescence stained 2-D gel in Figure 3 is identical to the spot indicated by the arrowhead in Figure 6.

Stathmin is also a phosphoprotein involved in the regulation of the cell cycle [22]. Four isoforms of stathmin, which correspond to phosphorylated forms [23,24], were clearly observed 6 h after exposure to oxLDL (Figure 7, indicated as arrowheads) but not in the controls. The disappearance of these phosphorylated isoforms and a decrease in the level of unphosphorylated stathmin (Figure 5) were observed after 24 h. This decreased expression may result in the suppression of cell proliferation.

Nucleolin, another cell proliferation-related protein, was detected as a 20-kDa truncated form on 2-D gel (Figure 3, Table I). The function of nucleolin may be regulated by post-translational modifications, most notably phosphorylation [25]. However, we observed no obvious nucleolin isoform in 2-D western blot analysis (data not shown). Instead, a 76-kDa nucleolin band corresponding to intact nucleolin was detected by western blot analysis of one-dimensional SDS-PAGE (Figure 8). The 76-kDa form of nucleolin decreased after exposure to oxLDL but not after exposure to intact LDL. The suppression of cellular proliferation was strongly associated with these modifications of the proteins mentioned above after exposure to oxLDL.

Discussion

LDL is composed of a surface layer containing phospholipids and free cholesterol and an inner core of cholesterol ester and triglycerides, with one macromolecule of apolipoprotein B-100. The oxidation of LDL with a water-soluble radical initiator has the advantage that the radical initiator can be easily removed from oxLDL by dialysis, whereas, metal ions such as copper cannot be removed because they bind to protein. oxLDL has dual effects on endothelial cells: Inducing cell proliferation at low concentrations, and inhibiting their proliferation at higher concentrations [26,27]. We observed significant suppression of proliferation by exposure to oxLDL as 25 μM hydroperoxides and hydroxides (100 μg LDL protein/ml). When oxLDL was applied to HUVEC, concomitant accumulations of CEOOH and CEOH in HUVEC was observed, but at amounts

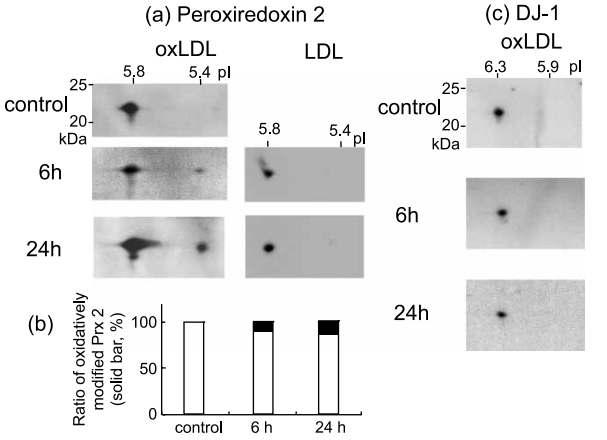

Figure 4. Western blot analysis of 2-D gel-separated proteins obtained from HUVEC exposed to oxidized LDL (oxLDL) for the indicated times. Peroxiredoxin 2 (Prx2) (A) and DJ-1 (C) spots were detected with specific antibodies. oxLDL was added to the cell culture medium at a final concentration of 25 μM hydroperoxides and hydroxides. In panel (A), the control result (exposure to an amount of intact LDL equivalent to the protein in oxLDL) is also shown in the right lane. A spot of oxidatively modified Prx2 (pI = 5.4) was detected and the ratio (oxidatively modified Prx2/total Prx2, %) is plotted as the black bar, in (B).

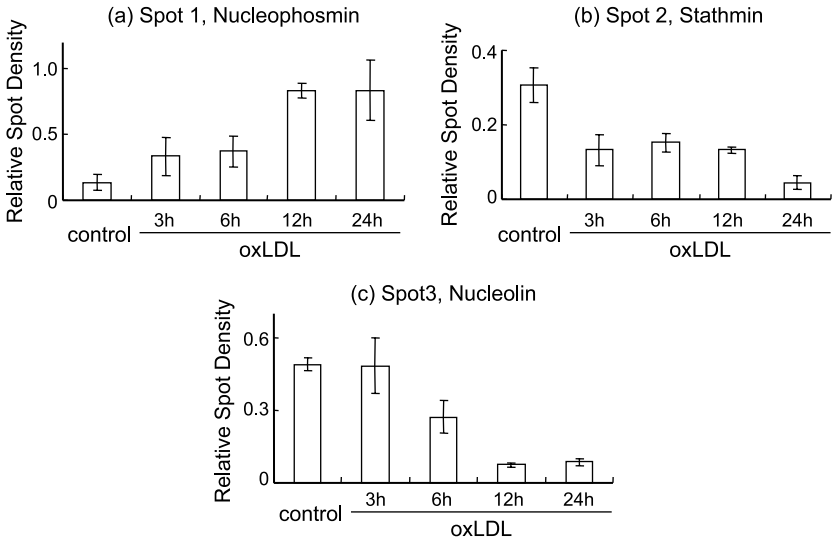

Figure 5. The relative spot densities of nucleophosmin (A), stathmin (B), and nucleolin (C) in HUVEC after exposure to oxidized LDL at a final concentration of 25 μM hydroperoxides and hydroxides. These protein spots correspond to those indicated in Figure 3. The normalized and averaged data are shown as relative density, means ± SD ($n = 3$).

that were less than 20% of the applied hydroperoxides and hydroxides. The accumulation of 7-KCh may be ascribed, at least in part, to the peroxidation of the free cholesterol present initially in HUVEC, induced by radicals formed by the decomposition of hydroperoxides. On the other hand, we used both Prx2 and DJ-1 as intracellular oxidative stress markers, which have different sensitivities to hydroperoxides [11,19]. Marked formation of oxPrx2 was observed by western blot analysis. However, no oxidative modification of DJ-1 was observed, perhaps due to the low response of DJ-1 to lipid hydroperoxides *in vivo*. Oxidative modification of Prx2 was observed concomitantly with the accumulation of 7-KCh in cells, suggesting that they are candidate of oxidative stress markers in this system.

We found three specific protein spots on fluorescence stained 2-D gel, which showed the different expression profiles induced in a time-dependent manner by exposure to oxLDL. We observed for the first time, as far as we can ascertain, that the expression of the three proteins, nucleophosmin, stathmin, and nucleolin, was altered by treatment with oxLDL. We further confirmed the post-translational modification of these proteins by western blot analysis. Nucleophosmin (formally named B23), which is involved in nucleolar assembly, centrosome duplication, and ribosome assembly and transport, is a known phosphoprotein. The phosphorylation sites have been partially determined at Ser-125, which is phosphorylated by casein kinase II [28], and at Thr-199 [29], Thr-234, and Thr-237 [30], which are phosphorylated by Cdk2 (cell division cycle protein-2) during mitosis. The hyperphosphorylation of nucleophosmin is enhanced in actively dividing tumor-derived cell lines compared with that in melanocytes [22]. In this study, a series of spots corresponding to the

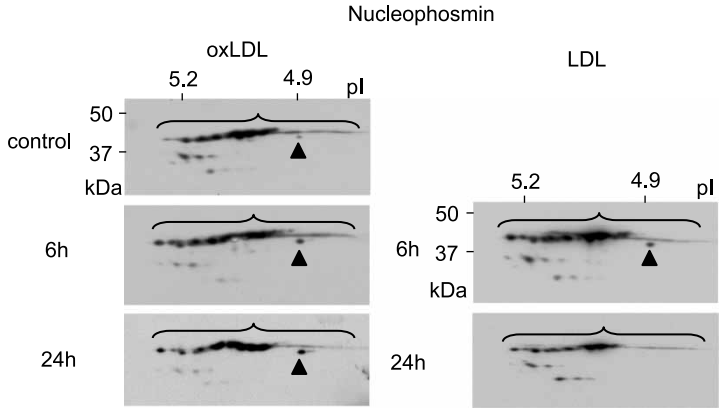

Figure 6. Western blot analysis of 2-D gel-separated proteins obtained from HUVEC exposed to oxidized LDL (oxLDL) for the indicated times. Nucleophosmin spots were detected with nucleophosmin-specific antibody. oxLDL was added to the cell culture medium at a final concentration of 25 μM hydroperoxides and hydroxides (left lane). The amount of intact LDL (LDL) added to the cell culture medium was equivalent to the protein added as oxLDL (right lane). Brackets show the series of nucleophosmin isoforms discussed in the text. Arrowhead shows another isoform of nucleophosmin that is identical to spot 1 in Figure 3.

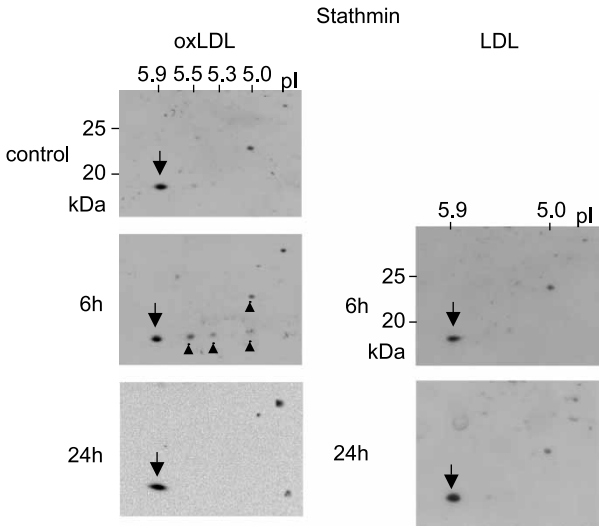

Figure 7. Western blot analysis of 2-D gel-separated proteins obtained from HUVEC exposed to oxidized LDL (oxLDL) for the indicated times. Stathmin spots were detected with stathmin-specific antibody. oxLDL was added to the cell culture medium at a final concentration of 25 μM hydroperoxides and hydroxides (left lane). The amount of intact LDL (LDL) added to the cell culture medium was equivalent to the protein added as oxLDL (right lane). The spot indicated by the arrow is an unphosphorylated form of stathmin that is identical to spot 2 in Figure 3. Arrowheads show the phosphorylated forms of stathmin.

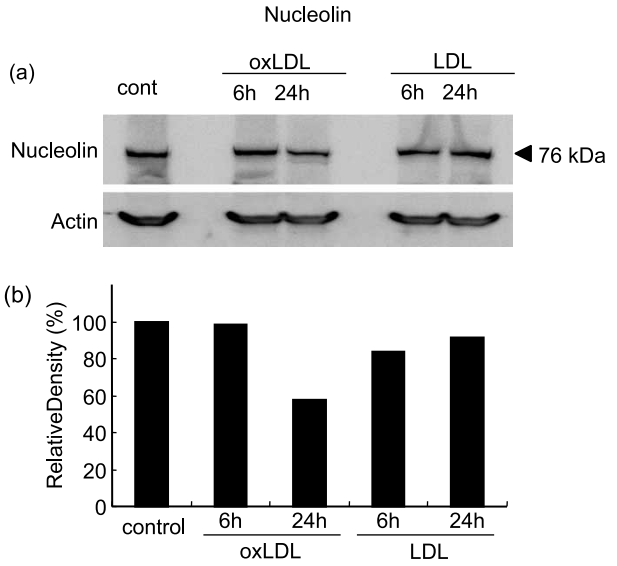

Figure 8. (A) Western blot analysis of SDS-PAGE-separated proteins obtained from HUVEC exposed to oxidized LDL (oxLDL) for the indicated times. Nucleolin bands were detected with nucleolin-specific antibody. oxLDL was added to the cell culture medium at a final concentration of 25 μM hydroperoxides and hydroxides. The amount of intact LDL (LDL) added to the cell culture medium was equivalent to the protein added as oxLDL. The blot was reprobed with actin-specific antibody. (B) The relative densities of bands after exposure to oxLDL and LDL compared with those of the control.

hyperphosphorylated nucleophosmin isoforms was observed, as indicated by the brackets in Figure 6. Furthermore, the dephosphorylation of this series of nucleophosmin spots was observed in a time-dependent manner after exposure to oxLDL. This observation may explain that the cell proliferation function is suppressed by exposure to oxLDL. On the other hand, the expression of one isoform of nucleophosmin, indicated by an arrowhead in Figure 6, increased. However, its structure is currently unknown. The implications of this observation should be clarified in future.

Stathmin (formally named oncoprotein 18/Op18) is a widely expressed, cell cycle-regulated phosphoprotein involved in microtubule dynamics. Stathmin is a major microtubule-destabilizing protein that causes the destabilization of growing microtubules and its phosphorylation inactivates this microtubule destabilizing activity [31]. The phosphorylation is induced by a variety of stimuli and during mitosis. For example, phorbol 12-myristate 13-acetate (PMA) treatment induced a rapid increase in several phosphorylated forms of stathmin in Jurkat cells [32]. HNE increased the phosphorylation of stathmin in PC-12 cells, whereas oxidized very low-density lipoprotein (VLDL) reduced its phosphorylation and inhibited cell proliferation [33]. Stathmin is phosphorylated at up to four residues, and the unphosphorylated, mono-, di-, tri-, and tetra-phosphorylated stathmins have been mapped on 2-D gel [24,25]. Our data clearly demonstrate that the four phosphorylated forms of stathmin were remarkably elevated 6 h after exposure to oxLDL. However, the phosphorylated forms had disappeared after 24 h. This observation may be interpreted as the phosphorylation of stathmin by the stimulus of oxLDL at 6 h. At this early stage, the phosphorylation of stathmin may be transiently responsible for the cellular stress response, as is the case for PMA and HNE mentioned above. However, the decreased level of unphosphorylated stathmin may be implicated in its proteasome-mediated degradation [34] and the subsequent suppression of cell growth [35].

Nucleolin is the major nucleolar phosphoprotein in exponentially growing eukaryotic cells and is a specific marker of angiogenic endothelial cells within the vasculature [36]. The intact 105-kDa nucleolin molecule is the major species in actively dividing cells and the stability of nucleolin is considered to be dependent on cell proliferation [37]. In non-dividing cells, nucleolin undergoes autodegradation to produce a series of fragments of the intact molecule. In this work, the 76-kDa fragment of nucleolin was detected by western blot analysis of HUVEC treated and untreated with oxLDL. The molecular weight of human nucleolin deduced from the database is 76,224, suggesting that the 76-kDa band was not post-translationally modified. We observed no nucleolin fragment apart from the 76-kDa band in this

western blot analysis. A decrease in the density of the 20-kDa nucleolin fragment was observed on 2-D gel after exposure to oxLDL, suggesting that the degradation of nucleolin in HUVEC caused by oxLDL exposure may be related to the suppression of cell growth.

In conclusion, the oxLDL used in this work stimulated HUVEC, resulting in the suppression of cell proliferation. The oxidative stress imposed on HUVEC was reflected in the accumulation of oxidized lipids and the oxidation of Prx2. Protein modifications, such as phosphorylation and autodegradation, and/or the altered expression of the proteins examined in this work were also induced under these oxidative stress conditions. Further study should help to discern whether the effects of oxLDL and the proteins investigated in this study are relevant under physiological conditions. Finally, it should be emphasized that the proteomic study presented here is a useful tool with which to understand the extensive mechanisms underlying atherosclerosis.

Acknowledgements

We thank Dr. Masayuki Kubota at Thermo Electron K.K. for technical assistance. This work was supported by grants from the Ministry of Education, Science, Technology and Culture of Japan.

References

[1] Halliwell B, Gutteridge JMC. Free Radicals in Biology and Medicine. 3rd ed. Oxford: Oxford University Press; 1999.
[2] Steinberg D, Witztum JL. Is the oxidative modification hypothesis relevant to human atherosclerosis? Circulation 2002;105:2107–2111.
[3] Zettler ME, Prociuk MA, Austria JA, Massaeli H, Zhong G, Pierce GN. OxLDL stimulates cell proliferation through a general induction of cell cycle proteins. Am J Physiol Heart Circ Physiol 2003;284:644–653.
[4] Maziere C, Djavaheri MM, Frey FV, Delattre J, Maziere JC. Copper and cell-oxidized low-density lipoprotein induces activator protein 1 in fibroblasts, endothelial and smooth muscle cells. FEBS Lett 1997;409:351–356.
[5] Kusuhara M, Chait A, Cader A, Berk BC. Oxidized LDL stimulates mitogen-activated protein kinases in smooth muscle cells and macrophages. Arterioscler Thromb Vasc Biol 1997; 17:141–148.
[6] Takahashi M, Okazaki H, Ogata Y, Takeuchi K, Ikeda U, Shimada K. Lysophosphatidylcholine induces apoptosis in human endothelial cells through a p38-mitogen-activated protein kinase-dependent mechanism. Atherosclerosis 2002; 161:387–394.
[7] Lizard G, Moisant M, Cordelet C, Monier S, Gambert P, Lagrost L. Induction of similar features of apoptosis in human and bovine vascular endothelial cells treated by 7-ketocholesterol. J Pathol 1997;183:330–338.
[8] Herbst U, Toborek M, Kaier S, Mattson MP, Hennig B. 4-Hydroxynonenal induces dysfunction and apoptosis of cultured endothelial cells. J Cell Physiol 1999;181:295–303.
[9] Rabilloud T, Heller M, Rigobello MP, Bindoli A, Aebersold R, Lunardi J. The mitochondrial antioxidant defence system and its response to oxidative stress. Proteomics 2001;1:1105–1110.
[10] Mitsumoto A, Takanezawa Y, Okawa K, Iwamatsu A, Nakagawa Y. Variants of peroxiredoxins expression in response to hydroperoxide stress. Free Radic Biol Med 2001;30:625–635.
[11] Mitsumoto A, Nakagawa Y, Takeuchi A, Okawa K, Iwamatsu A, Takanezawa Y. Oxidized forms of peroxiredoxins and DJ-1 on two-dimensional gels increased in response to sublethal levels of paraquat. Free Radic Res 2001;35:301–310.
[12] Wagner E, Luche S, Penna L, Chevallet M, Van Dorsselaer A, Leize-Wagner E, Rabilloud T. A method for detection of overoxidation of cysteines: peroxiredoxins are oxidized *in vivo* at the active-site cysteine during oxidative stress. Biochem J 2002;366:777–785.
[13] Fach EM, Garulacan LA, Gao J, Xiao Q, Storm SM, Dubaquie YP, Hefta SA, Opiteck GJ. *In vitro* biomarker discovery for atherosclerosis by proteomics. Mol Cell Proteomics 2004;3: 1200–1210.
[14] Fuchs D, De Pascual-Teresa S, Rimbach G, Virgili F, Ambra R, Turner R, Daniel H, Wenzel U. Proteome analysis for identification of target proteins of genistein in primary human endothelial cells stressed with oxidized LDL or homocysteine. Eur J Nutr 2005;44:95–104.
[15] Fuchs D, Erhard P, Turner R, Rimbach G, Daniel H, Wenzel U. Genistein reverses changes of the proteome induced by oxidized-LDL in EA-hy 926 human endothelial cells. J Proteome Res 2005;4:369–376.
[16] Ramos P, Gieseg SP, Schuster B, Esterbauer H. Effect of temperature and phase transition on oxidation resistance of low density lipoprotein. J Lipid Res 1995;36:2113–2128.
[17] Yoshida Y, Itoh N, Saito Y, Hayakawa M, Niki E. Application of water-soluble radical initiator. 2,2′-azobis[2-(2-imidazolin-2-yl)propane] dihydrochloride, to a study of oxidative stress. Free Radic Res 2004;38:375–384.
[18] Thomas JP, Kalyanaraman B, Girotti AW. Involvement of preexisting lipid hydroperoxides in Cu(2+)-stimulated oxidation of low-density lipoprotein. Arch Biochem Biophys 1994;315:244–254.
[19] Kinumi T, Kimata J, Taira T, Ariga H, Niki E. Cysteine-106 of DJ-1 is the most sensitive cysteine residue to hydrogen peroxide-mediated oxidation *in vivo* in human umbilical vein endothelial cells. Biochem Biophys Res Commun 2004;317:722–728.
[20] Rabilloud T, Heller M, Gasnier F, Luche S, Rey C, Aebersold R, Benahmed M, Louisot P, Lunardi J. Proteomics analysis of cellular response to oxidative stress. Evidence for *in vivo* overoxidation of peroxiredoxins at their active site. J Biol Chem 2002;277:19396–19401.
[21] Bernard K, Litman E, Fitzpatrick JL, Shellman YG, Argast G, Polvinen K, Everett AD, Fukasawa K, Norris DA, Ahn NG, Resing KA. Functional proteomic analysis of melanoma progression. Cancer Res 2003;63:6716–6725.
[22] Cassimeris L. The oncoprotein 18/stathmin family of microtubule destabilizers. Curr Opin Cell Biol 2002;14:18–24.
[23] Mueller DR, Schindler P, Coulot M, Voshol H, van Oostrum V. Mass spectrometric characterization of stathmin isoforms separated by 2-D PAGE. J Mass Spectrom 1999;34:336–345.
[24] Daub H, Gevaert K, Vandekerckhove J, Sobel A, Hall A. Rac/Cdc42 and p65PAK regulate the microtubule-destabilizing protein stathmin through phosphorylation at serine 16. J Biol Chem 2001;276:1677–1680.
[25] Peter M, Nakagawa J, Doree M, Labbe JC, Nigg EA. Identification of major nucleolar proteins as candidate mitotic substrates of cdc2 kinase. Cell 1990;60:791–801.
[26] Chen CH, Jiang W, Via DP, Luo S, Li TR, Lee YT, Henry PD. Oxidized low-density lipoproteins inhibit endothelial cell proliferation by suppressing basic fibroblast growth factor expression. Circulation 2000;101:171–177.
[27] Galle J, Heinloth A, Wanner C, Heermeier K. Dual effect of oxidized LDL on cell cycle in human endothelial cells through oxidative stress. Kidney Int Suppl 2001;78:S120–S123.

[28] Chan PK, Aldrich M, Cook RG, Busch H. Amino acid sequence of protein B23 phosphorylation site. J Biol Chem 1986;261:1868–1872.

[29] Tokuyama Y, Horn HF, Kawamura K, Tarapore P, Fukasawa K. Specific phosphorylation of nucleophosmin on Thr(199) by cyclin-dependent kinase 2-cyclin E and its role in centrosome duplication. J Biol Chem 2001;276:21529–21537.

[30] Cha H, Hancock C, Dangi S, Maiguel D, Carrier F, Shapiro P. Phosphorylation regulates nucleophosmin targeting to the centrosome during mitosis as detected by cross-reactive phosphorylation-specific MKK1/MKK2 antibodies. Biochem J 2004;378:857–865.

[31] Niethammer P, Batiaens P, Karsenti E. Stathmin-tubulin interaction gradients in motile and mitotic cells. Science 2004; 303:1862–1866.

[32] Wang YK, Liao PC, Allison J, Gage DA, Andrews PC, Lubman DM, Hanash SM, Strahler JR. Phorbol 12-myristate 13-acetate-induced phosphorylation of Op18 in Jurkat T cells. Identification of phosphorylation sites by matrix-assisted laser desorption ionization mass spectrometry. J Biol Chem 1993;268:14269–14277.

[33] Yamashita H, Nakamura K, Arai H, Furumoto H, Fujimoto M, Kashiwagi S, Morimatsu M. Electrophoretic studies on the phosphorylation of stathmin and mitogen-activated protein kinases in neuronal cell death induced by oxidized very-low-density lipoprotein with apolipoprotein E. Electrophoresis 2002;23:998–1004.

[34] Liu Z, Lu H, Shi H, Du Y, Yu J, Gu S, Chen X, Liu KJ, Hu CA. PUMA overexpression induces reactive oxygen species generation and proteasome-mediated stathmin degradation in colorectal cancer cells. Cancer Res 2005;65:1647–1654.

[35] Nakamura K, Fujimoto M, Tanaka T, Fujikura Y. Differential expression of nucleophosmin and stathmin in human T lymphoblastic cell lines, CCRF-CEM and JURKAT analyzed by two-dimensional gel electrophoresis. Electrophoresis 1995;16:1530–1535.

[36] Christian S, Pilch J, Akerman ME, Porkka K, Laakkonen P, Ruoslahti E. Nucleolin expressed at the cell surface is a marker of endothelial cells in angiogenic blood vessels. J Cell Biol 2003;163:871–878.

[37] Chen CM, Chiang SY, Yeh NH. Increased stability of nucleolin in proliferating cells by inhibition of its self-cleaving activity. J Biol Chem 1991;266:7754–7758.